ANALYSIS AND MEASUREMENT OF ELECTRIC FIELD EXPOSURE INSIDE 500/220 KV AIR INSULATED SUBSTATION

Essam M. SHAALAN.
Ass. Lec.: Elec. Power Dep., Faculty of Eng. at shoubra, benha university.
Cairo, Egypt.
essam.shihata@feng.bu.edu.eg

Samy M. GHANIA.
Ass. Prof.: Elec. Power Dep., Faculty of Eng. at shoubra, benha university.
Cairo, Egypt.
samy_ghania@yahoo.com

Syed A. WARD.
Prof.: Elec. Power Dep., Faculty of Eng. at shoubra, benha university.
Cairo, Egypt.
drsayedw@yahoo.com

Abstract*—the possible effect of low frequency electric field exposure in occupational and residential environments raises the question of how electric fields are created, and what effects they may have. Utilities in particular are interested in the sources and levels of electric fields associated with their transmission lines, feeders, substations and related equipments. Moreover the value of electric field distribution produced by or around the electrical equipments is one of the essential factors in the design and development of high voltage electrical equipments (transmission lines, bus bars & insulators….etc). Therefore monitoring these equipments for electric fields is achieved in this paper. In this paper not only the simulation of electric field using charge simulation method (CSM) in three dimensional (3-D) is achieved by using electric field modeling program developed by the authors but also the electric field is measured into actual conventional 500/220 kV Cairo 500 substation under 500 kV busbar and the simulated results is compared with the actual measured values. The simulation results are matched with the measured values with a very small tolerance about 4.4%.*

Keywords- *electric field, high voltage substation, charge simulation method.*

I. INTRODUCTION

During the last two decades, the electric fields have been considered more and more environmental factors while the National standards define the maximum values of the electric field strength for occupational and general public exposure (occupational period of stay is eight hours per day and general public period of stay is twenty four hours per day) as 10 kV/m for the occupational exposure and 5 kV/m for the public exposure [1,2]. Therefore, the electric field calculation is one of the essential factors in the design and development of any electrical utilities to guarantee the life insurance of their workers [3-19]. The electric field is usually calculated with the use of several numerical methods through a computer. The charge simulation method is one of these numerical methods which used commonly for engineering applications to compute successfully and accurately the electric field [20]. Therefore in this paper the charge simulation method is used to simulate the three dimensional electric field by using the modeling program developed by the authors [21,22]. This paper presents the results of measurement and simulation of the electric fields on a typical 500/220 kV substation (Cairo 500 air insulated substation located in the west of Cairo. A simple representation and description for this substation will be presented and different cases of study will be demonstrated on the values of the electric field such as; the steady state operation or normal operation, the current interruption in one or more outgoing or incoming circuits due to the load condition, the effect of changing the level of calculation and finally the effect of changing the space between the phases. Moreover, the electric field is measured into this substation under 500 kV busbar using the field meter device (*HI 3604 ELF survey meter*) and the simulated results are compared with the actual measured values.

II. SUBSTATION DESCRIPTION AND SYSTEM MODELING

The analyzed 500/220 kV outdoor air insulated substation is supplied by four 500 kV overhead transmission lines (the first line is feeding from Al-korimat power station, the second line is feeding from Samaloot power station, the third line is feeding from Al-Nobariea power station, the fourth line is feeding from Cairo west power station) which are connected to the same main bus system and a bypass bus system. This substation has three identical 3-phase power transformers installed inside it, each transformer is composed of three single phase transformers and has rated of 500 MVA and 500/220/11 kV. Each conductor's phase of 500 kV or 220 kV bus system, incoming, and outgoing feeders consist of double circuit. This substation has a simply 500 kV bus system with 300 m long and 12 m height above the earth. The 3-D spatial model, with elements used in the field calculation inside this substation is shown in Fig. 1.

For evaluating the electric field produced inside this substation, the three-dimensional model of 500kV switchyard inside this substation has been developed including the incoming and outgoing conductors, bus system, HV apparatus, fences and the towers [22].

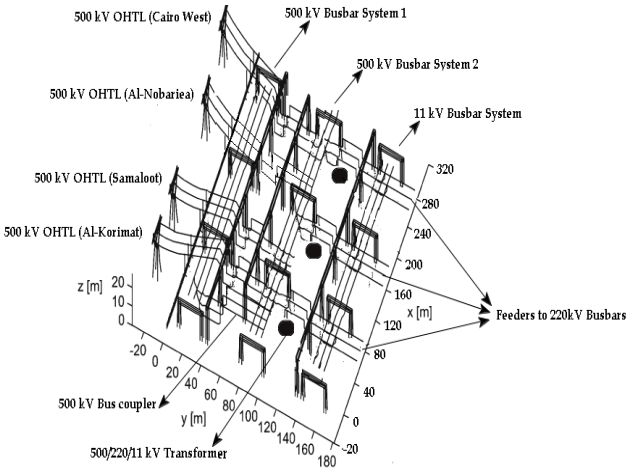

Figure 1. 3-D spatial model of 500 kV switchyard inside Cairo 500 substation.

The 500 kV bus system is modeled as continuous elements connected throughout the substation by means of breakers and isolators (*disconnectors*) without any isolated sections. The earth mat was not modeled as balanced (current) conditions were assumed. Fig. 2 shows a simple presentation of the model considered for 500kV switchyard to calculate the electric field into this area.

III. ELECTRIC FIELD CALCULATION METHODOLOGY FOR MODELS UNDER STUDY

The basic principle of CSM lies in replacing the surface charge of the conductor with a set of discrete fictitious charges located inside the conductor. These fictitious charges generate the electric field of similar intensity and direction as the original conductors in the observed zone. For the present developed model, the fictitious linear charges are used for the modeling of the line conductors (phase conductors, main bus system, and bypass system) with a certain arrangement [21,22].

Although the type and position of these fictitious charges inside the conductors are specified in advance [21,22], their values are unknown and in order to determine the value of these fictitious charges of the number (n_s) on the conductor with known potential (V_{con}), a certain number (n_{cp}) of contour points are selected where the condition ($n_s = n_{cp}$) is satisfied. The contour points are placed at the conductor surface where the boundary conditions given by potentials of the contour points equal to V_{con} are satisfied ($V_{cp}=V_{con}$). After choosing the type of fictitious charges as linear finite line type and distributing them along the simulated conductors, The values of these discrete charges are determined by satisfying the boundary conditions in (1) at a selected number of contour points where the potentials of these fictitious charges are taken as particular solutions of Laplace equation which governs the assessment of the electric field.

$$[V] = [P]\,[Q] \tag{1}$$

Where: [Q] is a column vector of the fictitious simulation charges, [V] is a column vector of the potential given by the boundary conditions and [P] is the matrix of the Maxwell potential coefficients [20, 23].

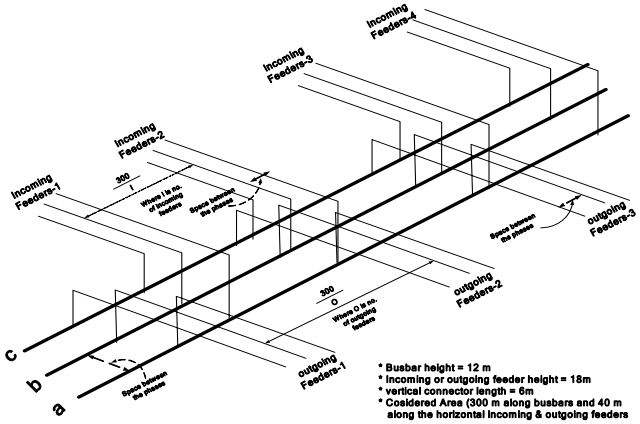

Figure 2. The considered 500 kV switchyard to calculate the electric field inside Cairo 500 substation.

Consider a finite line charge with constant charge densities (*Total charge* Q_j) of length (d) with both ends at (X_1, Y_1, Z_1) as end point and (X_2, Y_2, Z_2) as starting point as shown in Fig. 3, then the potential coefficient (P_{ij}) at any point P_i (X, Y, Z) due to this charge and its image charge ($-Q_j$) with respect to the plane is given as following:

$$P_{ij} = \frac{1}{4\pi\varepsilon d}\ln\left\{\frac{(L_1 + L_2 + d)(L_{11} + L_{22} - d)}{(L_1 + L_2 - d)(L_{11} + L_{22} + d)}\right\} \tag{2}$$

Where

$$L_1 = \sqrt{(X-X_1)^2 + (Y-Y_1)^2 + (Z-Z_1)^2}$$
$$L_2 = \sqrt{(X-X_2)^2 + (Y-Y_2)^2 + (Z-Z_2)^2}$$
$$L_{11} = \sqrt{(X-X_1)^2 + (Y-Y_1)^2 + (Z+Z_1)^2}$$
$$L_{22} = \sqrt{(X-X_2)^2 + (Y-Y_2)^2 + (Z+Z_2)^2}$$
$$d = \sqrt{(X_1-X_2)^2 + (Y_1-Y_2)^2 + (Z_1-Z_2)^2}$$

After the calculation of the values of these charges, the potential is calculated at check points to satisfy the boundary condition at check points (different from boundary points) and to check the error tolerance which has to be minimized for satisfactory determination of charges and if the calculation accuracy isn't satisfied, there are two ways to improve the accuracy of calculation; the first relates to the proper selection of the types and the number of simulated charges, and the second to the suitable arrangement of simulated charges

and contour points. As soon as an adequate charge system has been developed, the potential and the field at any point can be calculated while the value of the potential and the electric field can be calculated by superposition of magnitudes of various directional components.

The expression for the field coefficients (F) in the x, y and z directions due to this finite line charge (Q_j) and its image charge (- Q_j) at contour point (P_i) are given as following:

$$F_x = \frac{1}{4\pi\varepsilon d}\left\{\left(\frac{X-X_1}{L_1}+\frac{X-X_2}{L_2}\right)\Gamma 1-\left(\frac{X-X_1}{L_{11}}+\frac{X-X_2}{L_{22}}\right)\Gamma 2\right\} \quad (3)$$

$$F_y = \frac{1}{4\pi\varepsilon d}\left\{\left(\frac{Y-Y_1}{L_1}+\frac{Y-Y_2}{L_2}\right)\Gamma 1-\left(\frac{Y-Y_1}{L_{11}}+\frac{Y-Y_2}{L_{22}}\right)\Gamma 2\right\} \quad (4)$$

$$F_z = \frac{1}{4\pi\varepsilon d}\left\{\left(\frac{Z-Z_1}{L_1}+\frac{Z-Z_2}{L_2}\right)\Gamma 1-\left(\frac{Z+Z_1}{L_{11}}+\frac{Z+Z_2}{L_{22}}\right)\Gamma 2\right\} \quad (5)$$

Where

$$\Gamma 1 = \frac{1}{(L_1+L_2-d)}-\frac{1}{(L_1+L_2+d)} \qquad \Gamma 2 = \frac{1}{(L_{11}+L_{22}-d)}-\frac{1}{(L_{11}+L_{22}+d)}$$

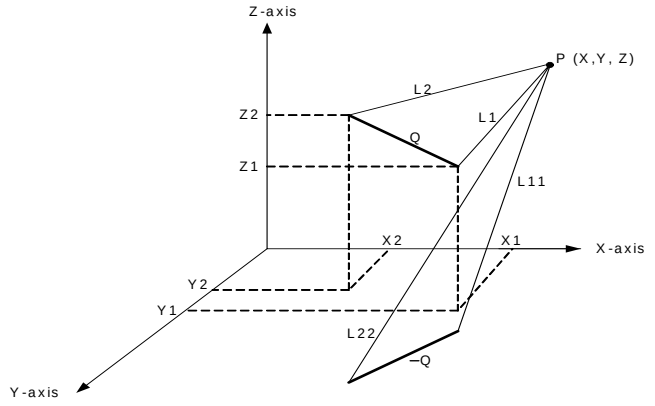

Figure 3. Finite line charge with constant charge densities and contour point P_i in three dimensional; in x, y and z directions.

The superposition theorem is applied to calculate the electric field strength at point i, in the function of complex fictitious charges placed at point j:

$$E_{xi} = \sum_{j=1}^{n} F_{xij} \times Q_j \quad (6)$$

$$E_{yi} = \sum_{j=1}^{n} F_{yij} \times Q_j \quad (7)$$

$$E_{zi} = \sum_{j=1}^{n} F_{xij} \times Q_j \quad (8)$$

Where E_{xi}, E_{yi}, E_{zi} are complex components of the electric field strength, in the *x*, *y* and *z*-directions respectively, *n* is the number of observed fictitious charges, F_{xij}, F_{yij}, F_{zij} are complex components of field coefficients of finite line fictitious charges [24].

After the calculation of the electric field strength in a three-phase system of sinusoidal low-frequency voltages, the root means square value of the electric field strength is proportional to the rms value of the voltages at all conductors. The total complex value of the electric field strength ($\underline{E}_{ti}$) is obtained by summing vector components E_{xi}, E_{yi} and E_{zi}.

$$\underline{E}_{ti} = E_{xi} * \underline{a}_x + E_{yi} * \underline{a}_y + E_{zi} * \underline{a}_z \quad (9)$$

Where $\underline{a}_x$, $\underline{a}_y$ and $\underline{a}_z$ are unit vectors in the x, y and z directions respectively.

The effective value of the electric field in the i^{th} observed point is calculated as the rms value within a single period. Finally the CSM equations mentioned above are generalized in the form of many Matlab M-files programs with the same sequence found in flowchart shown in Fig. 4 to simulate and calculate the electric field distribution underneath and around the 500kV bus system inside the investigated substation.

IV. THE SIMULATION RESULTS AND DISCUSSION

A. Steady State Operation or Normal Operation

Within the HV investigated substation, the measurements and the calculations of electric field were done along the 500 kV bus-system. Outside the HV substation, the measurements and the calculations were done in the zone near the protective fence of the substation, and below the overhead lines entering and leaving the substation. The calculation of the electric field strength is performed inside a 500 kV substation where the ground surface is included into the calculation by application of the so-called images method.

The bypass conductors, grounded conductors and dielectrics are neglected in this developed model in the selected substation and the modeling was done using 150 lineal segments of the line conductors connected to the network. The height of a typical worker (*human body*) is assumed to be 1.75 m [25]. Therefore the computation of electric field strength is performed at 1m above the ground surface inside the substation and in its vicinity along the 500 kV switchyard with length step of 7.5 m and presented as two dimensional (2-D) graphs as shown in Fig. 5 which display the distribution of the 2-D electric field strength along the 500 kV switchyard in the substation.

From this figure, it is found that for 12 m busbar height stressed at 500kV line voltage, the maximum calculated electric field strength values are 23.9, 21.3, 20.95 kV/m which exceed the International Commission

for Non-ionizing Radiation Protection (ICNIRP) reference level at three locations (under phase A of 500kV busbar at distance from 157.5 m to 172.5 m) covering a small area about 15 x 6 m in the HV switchyard. Also it was found that as the conductor phase of 500 kV busbar comes nearby the switchgear, the value of calculated electric field strength is decreased because the field cancellation factor is increased.

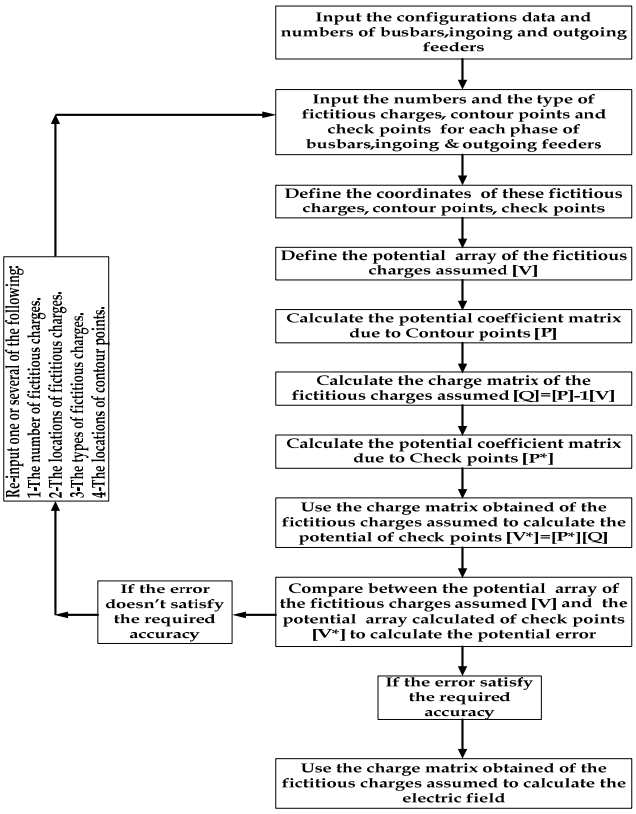

Figure 4. The flow chart of CSM methodology in 3-D to assessment the electric field inside HV substations.

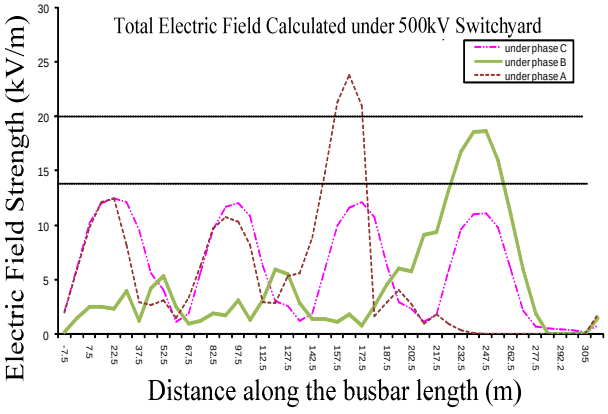

Figure 5. The 2-D electric field distribution under different phases of 500 kV busbar inside Cairo 500 substation.

Beside the above calculation of the electric field in two dimensional, the calculation of the 3-D electric field strength inside the substation and in its vicinity was performed in the switchyard area (300*40 m around and underneath the 500 kV bus system) with length step of 4 m and presented as 3-D graphs as shown in Fig. 6 which display the calculations results in the whole area of 500kV switchyard. From this figure, it is found that for 12 m busbar height and 18 m incoming and outgoing feeders height stressed at 500kV line voltage, the maximum calculated electric field strength value is 13.45 kV/m at a point P(x,y) = P(19,21) in the calculation grid at 1 m above the ground surface. Also the average value of the calculated electric field strength here is 4.91kV/m. it should be noted that the above 3-D calculations are performed when all incoming and outgoing feeders are turned on, at spacing between the phases of 6m, and at height level of calculation of 1 m (*the base case of our study*).

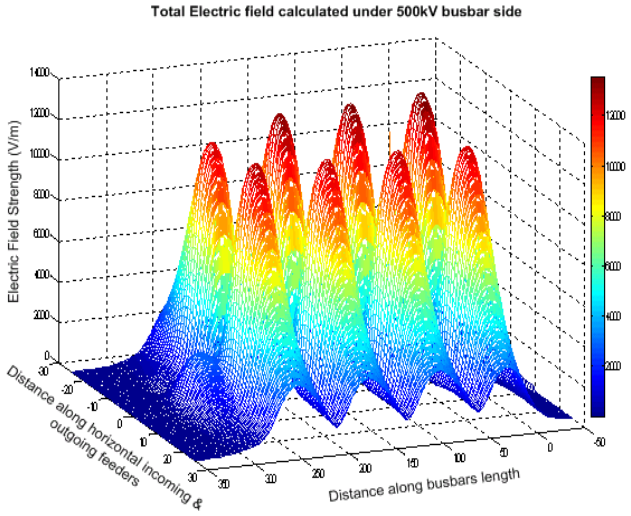

a) 3-D Distribution

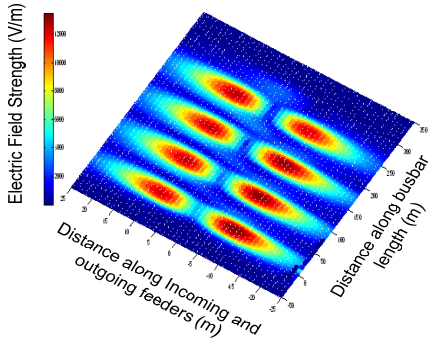

a) Contour Distribution

Figure 6. The 3-D electric field distribution in the 500 kV switchyard area inside Cairo 500 substation.

B. Changing the Space between the Phases

By decreasing the spacing between the phases to 5 m, the maximum value of the calculated 3-D electric field strength is decreased by 8.83% because the cancellation factor is increased, while the increasing of the spacing between the phases to 7 m will increase the maximum value of the calculated 3-D electric field strength by 8.04% because the cancellation factor is decreased as shown in Table 1. But it should be noted that while decreasing the space between the phases, it should keep the insulation between the phases with national standard for each operating voltage to prevent the breakdown occurrence.

TABLE 1. The Effect of The Spacing between the phases on The electric field calculation.

The Operating Voltage	The height level of Calculation (m)	The spacing between the phases (m)	Maximum Field Value (KV/m)	Average Field Value (KV/m)	Position of maximum field (x,y) in meter	The Field strength difference with respect to the base case
500 KV	1 m	6	13.45	4.91	P (x, y)= (19, 21)	Base Case
		5.8	13.2	4.7	P (x, y)= (56, 22)	decreased with 1.86%
		5.6	12.93	4.5	P (x, y)= (56, 22)	decreased with 3.86%
		5	12.26	4.32	P (x, y)= (56, 22)	decreased with 8.83%
		4	11.84	3.85	P (x, y)= (56, 22)	decreased with 11.95%
		6.2	13.7	5.1	P (x, y)= (19 , 21)	increased with 1.86%
		6.5	14.04	5.3	P (x, y)= (19 , 21)	increased with 4.39%
		7	14.53	5.46	P (x, y)= (19 , 21)	increased with 8.04%

B. *Changing the Level of Calculation*

By increasing the height level of calculation to 2 m or 3 m or 4 m, the maximum value of the calculated 3-D electric field strength is increased by 3.69%, 10.24% and 22.96% because of the closing from the live parts as shown in Table 2. Also it can be noted that we can decrease the maximum value of the calculated 3-D electric field strength by increasing the height level of supporting the live conductors (support the conductors at higher distance from the ground surface).

C. Changing The Load Condition

When the middle incoming feeder is switched off due to the load condition, the maximum value of electric field strength is increased by 3.72% because of decreasing the cancellation factor and the point of this maximum field is displaced from p(x,y) = P(19,21) to P(x,y) = P(56,21) as shown in Table 3.

TABLE 2. The Effect of changing the Height Level of Calculation on The electric field calculation.

The Operating Voltage	The spacing between the phases (m)	The height level of Calculation (m)	Maximum Field Value (KV/m)	Average Field Value (KV/m)	Position of maximum field (x,y) in meter	The Field strength difference with respect to the base case
500 KV	6 m	1	13.45	4.91	P (x, y)= (19, 21)	Base Case
		1.5	13.66	4.98	P (x, y)= (19 , 22)	increased with 1.56%
		1.75	13.79	5.07	P (x, y)= (19 , 22)	increased with 2.53%
		2	13.95	5.12	P (x, y)= (19 , 22)	increased with 3.72%
		3	14.83	5.38	P (x, y)= (19 , 22)	increased with 10.24%
		4	16.54	5.84	P (x, y)= (19, 22)	increased with 22.97%

TABLE 3. The Effect of Switching On/Off One or More Feeders on The electric field calculation.

The Condition	Maximum Field Value (KV/m)	Average Field Value (KV/m)	Position of maximum field (x,y) in meter	The Field strength difference with respect to the base case
Normal Operation	13.45	4.91	P (x, y)= (19, 21)	Base Case
Middle incoming feeder is switched off	13.95	4.99	P (x, y)= (56, 21)	increased with 3.72%
Two sides incoming feeders are switched off	14.07	5.05	P (x, y)= (37, 21)	increased with 4.57%
Middle outgoing feeder is switched off	13.93	5.13	P (x, y)= (74, 30)	increased with 3.51%
Two sides outgoing feeders are switched off	15.22	5.29	P (x, y)= (74 , 29)	increased with 13.13%
All outgoing feeders are switched off	16.78	5.55	P (x, y)= (74, 29)	increased with 24.75%

V. THE MEASUREMENT OF THE ELECTRIC FIELD INSIDE HV SUBSTATION

The electric field measurements are performed in this paper at 1m above the ground surface and nearby the 500 kV switchyard as shown in Fig. 7 using an advanced field meter in order to compare the simulated results and the actual measured field values [26,27]. Fig. 7 outlines the longitudinal electric field profiles measured under different phases of 500kV switchyard inside the substation, from this figure it is noticed that the maximum electric field value due to the different three phases is 22.9 kV/m and occurs at position x=190 m along the busbar length and located under phase C of 500kV busbar, while the minimum value is about 0.8 kV/m and located at position x=310 m along the busbar length and under phase C of 500 kV busbar. Also it is noticed that the electric field measured values are decreased as nearby from the 500kV switchgear; the electric field strength values under phase A (closer to 500 kV switchgear) are less than the corresponding values under phase C (most distance from 500 kV switchgear); due to the increasing of field cancellation factor. The maximum calculated value of electric field strength is 23.9kV/m while the maximum measured value is 22.9kV/m, therefore the simulation results are matched with the measured values with very small tolerance (about 4.4%).

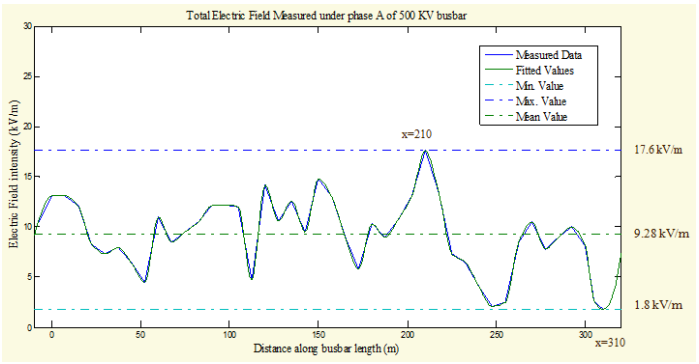

a) Under phase A

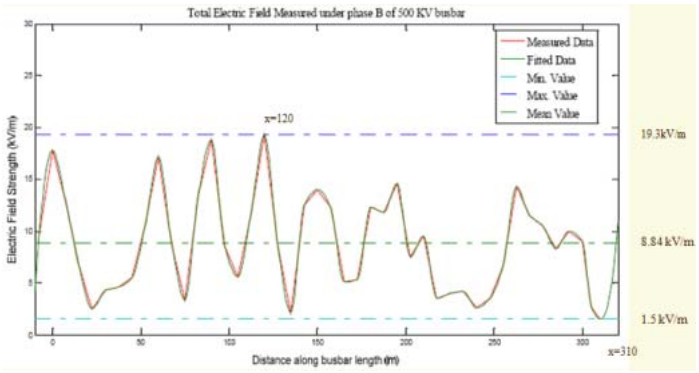

b) Under phase B

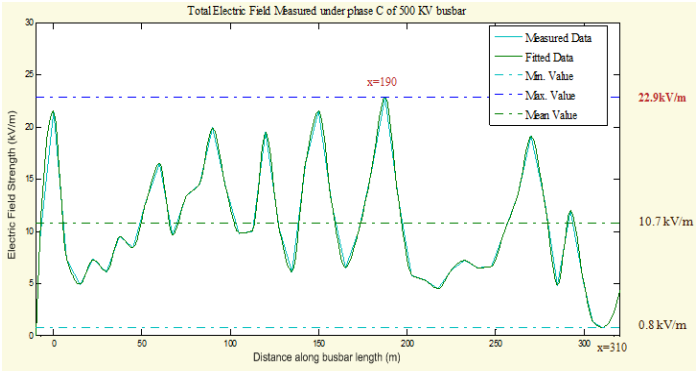

c) Under phase C

Figure 7. the longitudinal electric field profile measured under 500 kV switchyard inside cairo 500 substation at level 1m.

VI. THE CONCLUSION

From this study of the electric field distribution inside high voltage substations, we can conclude the following:

1. Following the electric field distribution inside air insulated substation (AIS), there are large areas especially in the 500 kV switchyard where the electric field intensity is higher than 10 kV/m; exceeds the professional exposure limit and the highest values have been found in the neighborhood of the incoming 500 kV transmission lines which are not encapsulated inside enclosures filled with SF_6 where the electric field strength under these lines reaches values up to 23kV/m; exceeds the professional exposure limit. The calculated and measured electric field around the fence of the substation is separated into three areas. In area I, the field is less than 5 kV/m, area III has less than 10 kV/m. The maximum is in the area II under the 500 kV transmission lines, which is greater than the limit for 24-hours exposure time for humans. Therefore the results presented show that the professional human exposure limit to the electric field is significantly exceeded in several areas of AIS especially under the 500 kV lines, busbars and around the power transformers. This is because of the circuit breakers and the disconnecting switches make the 500 kV potential to go down to 6.5 m above the ground.
2. On the 220 kV side of this substation, there are quit small areas where the electric field intensity exceeds the professional exposure limit which under the circuit breakers and disconnecting switches (reclosers).
3. Decreasing the space between the phases by centimeters will produce decreasing in the value of the electric field by hundreds of volt per meters because of increasing the contribution of the field cancellation factor, but when we increase the space between the phases by centimeters, the value of the electric field is increased by hundreds of volt per meters because of decreasing the contribution of the field cancellation factor. But we should be noted that while decreasing the space between the phases, it should keep the insulation between the phases with stated values by national standards for each operating voltage to prevent the breakdown occurrence.
4. As the height level of calculation is increased, the maximum value of the calculated field strength is increased because of closing from the live parts. This meaning also that as the height level for supporting the live conductors (busbars, incoming feeders and outgoing feeders) increased, the maximum value of the calculated field strength is decreased because of the distance from the live parts.
5. As the middle incoming feeder is switched off the maximum electric field value is increased by 3.72 % from base case; this is due to the reduction in the contribution of this feeder in the field cancellation factor. Besides that when all outgoing feeders are put off the maximum electric field value is increased by 24.75% from base case, this because the contribution of cancellation factor from all these lines are stopped and consequently a higher electric field value is obtained.
6. The electric field strength can be decreased to meet the National standards reference exposure levels by one from the following:
   - ❑ Increasing the height level of busbars, incoming feeders and outgoing feeders (live conductors) for example, particularly in 500 kV substations with proposed 12 m busbar height. If the ICNIRP levels are not met, the busbar height has to be increased to 14 m with significant cost implications.
   - ❑ Decreasing the space between the phases of busbars, incoming feeders and outgoing feeders (live conductors) but with a limit value to insure the insulation between them and prevent the occurrence of breakdown.
   - ❑ The live conductors (busbars, incoming feeders and outgoing feeders shall be housed in separate metal enclosed modules, called metal-clad switchgear, which filled with a superior dielectric gas; sulfur hexafluoride (SF_6) and this enclosure should be grounded.

REFERENCES

[1] International Commission on Non-Ionizing Radiation Protection, "*Guidelines for limiting exposure to time-varying electric, magnetic and electromagnetic fields (up to 300 GHz)*", Health Phys., vol. 74, no. 4, pp. 494–522, April 1998.

[2] IEEE Std. Safety Levels With Respect to *Human Exposure to Electromagnetic Fields, 0 to 3 kHz*, IEEE Std. C95.6-2002, Oct. 2002.

[3] Srete Nikolovski, Predrag Maric, Zoran Baus, "*Electromagnetic field calculation of transformer station 400/110kV ERNESTINOVO using the CDEGS software*", Journal of Electrical Engineering, vol. 58, no. 4, p-p. 207–213, 2007.

[4] Marinko STOJKOV, Damir SLJIVAC, Lajos JOZSA, "*Electric and magnetic field computation of 35 kV voltage level of transformer substation 35/10 kV using the CDEGS software*", Acta Electrotechnica et Informatica, vol. 10, no. 4, p-p. 64–68, 2010.

[5] Gh. Visan, I. T. Pop, C. Munteanu, "*Computation of the Electric and Magnetic Field Distribution inside High and Very High Voltage Substations*", the Online Journal on Electronics and Electrical Engineering (OJEEE), vol. 2, no. 2,p-p. 211-216, 2010.

[6] Karol GRABNER, Breda CESTNIK, "*Installation of new power substation in the environment with regard of Slovenian non-ionising radiation legislation*", 17th International Conference on Electricity Distribution (C I R E D), Session 2, Paper No 6, Barcelona, 12-15 May 2003.

[7] B. Trkulja, Z. Stih, "*Computation of Electric Fields inside Large Substations*", IEEE Transactions on Power Delivery, Vol. 24, no. 4, page 1898, Oct. 2009.

[8] Tang Ling Wang, Xiaoyu Qiao Liang, Sun Lu Yang Fan, "*Calculation of Power Frequency Electric Field in HV Substation Using BEM*", 2011 Asia-Pacific Power and Energy Engineering Conference (APPEEC), 25-28 March 2011.

[9] C. Munteanu, I.T. Pop, G. Visan, V. Topa, A. Racasan, M. Purcar, "*Analysis of the power frequency electric field generated by high voltage substations*", 2010 Asia-Pacific Symposium on Electromagnetic Compatibility (APEMC), 12-16 April 2010.

[10] W. Krajewski, "*Numerical modeling of the electric field in HV substations*", IEE Proceedings-Science, Measurement and Technology, vol. 151, no. 4, on page(s): 267, 2 July 2004.

[11] C. Munteanu, I.T. Pop, G. Visan, V. Topa, A. Racasan, "*Computation methods and experimental measurements of the electric and magnetic field distribution inside high voltage substations*", International Conference on Electromagnetics in Advanced Applications (ICEAA '09), 14-18 Sept. 2009.

[12] Poljak, Dragan Kovac, Niksa Gonzalez, Cristina Peratta, Andres Kraljevic, Sasa, "*Assessment of Human Exposure to Power Substation Electric Field*", 2006 International Conference on Software in Telecommunications and Computer Networks (SoftCOM), Sept. 2006.

[13] W.Joseph, L.Verloock, L. Martens, "*General Public Exposure by ELF Fields of 150–36/11-kV Substations in Urban Environment*" IEEE Transactions on Power Delivery, vol. 24 , no. 2, on page(s): 642, April 2009.

[14] J. Latva-Teikari, T. Karjanlahti, J. Kurikka-Oja, J. Elovaara, T. Langsjo, L. Korpinen, "*Measuring occupational exposure to electric and magnetic fields at 400 kV substations*", Transmission and Distribution Conference and Exposition, 21-24 April 2008.

[15] J. Isokorpi, T. Keikko, L. Korpinen, "*Power frequency electric fields at a 400 kV substation*", Eleventh International Symposium on High Voltage Engineering, 23-27 Aug 1999.

[16] Lu Binxian Wang Zezhong, Li Chengrong Ding Lijian, Wang Wei Zhang Weidong, "*The switching transient electric field measurements in a 500 kV substation*", 3rd International Symposium on Electromagnetic Compatibility, 21-24 May 2002.

[17] A.S. Safigianni, C.G. Tsompanidou, "*Measurements of electric and magnetic fields due to the operation of indoor power distribution substations*" , IEEE Transactions on Power Delivery, vol. 20 , no. 3, on page(s) 1800, July 2005.

[18] T. Sauramaki, T. Keikko, S. Kuusiluoma, L.Korpinen, "*Exposure to electric and magnetic fields at 110 kV gas insulated substation (GIS)*" , Asia Pacific. IEEE/PES Transmission and Distribution Conference and Exhibition, vol. 2, 6-10 Oct. 2002.

[19] P.S. Wong, T.M. Rind, S.M. Harvey, R.R. Scheer, "*Power frequency electric and magnetic fields from a 230 kV gas-insulated substation*", IEEE Transactions on Power Delivery, vol. 9 , no. 3, on page(s) 1494, Jul 1994.

[20] E.kuffel, W.S. Zaengle and J. Kuffel, "*High voltage engineering, fundamentals*", Newnes, Second edition reprint, 2001 (book).

[21] Essam M. Shaalan, Samy M. Ghania and Sayed A. Ward, "*Analysis of Electric Field inside HV Substations using Charge simulation method in three dimensional*", 2010 Annual Report Conference on Electrical Insulation and Dielectric Phenomena (CEIDP), October 2010.

[22] Essam M. Shaalan, "*Electric field calculation inside GIS using CSM in 3-D*", (M.Sc. thesis), faculty of engineering at shoubra, benha university, Egypt, 2011.

[23] Nazar H. Malik, "*A review of the charge simulation method and its applications*" IEEE Transactions on Electrical Insulation, vol. 24, no. 1, pp. 3–20, February 1989.

[24] Masanori Akazaki and Kiyoto Mishijima, "*Calculation of three dimensional axisymmetric fields by charge simulation method*", Electrical Engineering in Japan, vol. 98 no. 4, pp.1–7, July 1978.

[25] I.O. Habiballah, T. K. Abdel-Galil, M. M. Dawoud, C. A. Belhadj, M. Arif Abdul-Majeed, and T.A. Al-Betairi, " *ELF Electric and Magnetic Fields Exposure Assessment of Live-Line Workers for 132 kV Transmission Line of SEC*", IEEE PES Transmission and Distribution Conference and Exposition Latin America, Venezuela, pp. 1-6, 2006.

[26] HI 3604 ELF Survey Meter User's Manual, Holladay Ind. 2002.

[27] HI-4413 Fiber Optic RS-232 Interface With Probe View™ 3600 User's Manual.